Journal of Organometallic Chemistry 694 (2009) 2927–2933

Contents lists available at ScienceDirect

Journal of Organometallic Chemistry

journal homepage: www.elsevier.com/locate/jorganchem

Synthesis, ethylene polymerization and dynamic features of titanium and zirconium complexes bearing chelating malonate-based enaminoketonato ligands

Pertti Elo, Antti Pärssinen, Martin Nieger, Markku Leskelä, Timo Repo *

Department of Chemistry, Laboratory of Inorganic Chemistry, University of Helsinki, P.O. Box 55, 00014 Helsinki, Finland

ARTICLE INFO

Article history:
Received 16 January 2009
Received in revised form 16 April 2009
Accepted 21 April 2009
Available online 3 May 2009

Keywords:
Ti and Zr complexes
Dynamic NMR
Polymerization
(N,O)-ligands

ABSTRACT

Synthesis of new titanium and zirconium dichloro complexes bearing malonate-based enaminoketonato (N,O) ligand is described. NMR studies of the catalyst precursors reveal that synthesized complexes have different configurational isomers in solution state and that they undergo structural change within NMR timescale. After MAO activation complexes exhibited low to moderate activities in ethylene polymerization producing bi- or multimodal polyethylenes.

1. Introduction

Extensive research, both in academia and in industry, has been dedicated for the development of non-metallocene olefin-polymerization catalysts [1–6]. Group IV metal complexes with a wide range of heteroatom-donor ligands have been prepared and used as catalyst precursors in ethylene polymerization [7–19]. Complexes bearing (N,O)-type chelating ligands, like Fujita's FI-catalysts, and enaminoketonato-complexes, have attracted considerable interest [20–24]. These types of complexes have shown both high polymerization activities and interesting possibilities for example in the areas of living polymerization [25,26], co-polymerization [27,28] and polymerization of higher α-olefins [29].

The versatility of these complexes arises from the variation of the ligand structure which leads to significant changes in the catalytic activity and in the properties of the produced polymer products [28]. It has been also shown that in some cases enaminoketonato complexes are more active than the corresponding alkoxy-complexes [23–31]. This led us to develop new enaminoketonato complexes where the ligand-structure is based on malonate-ester backbone which we have previously used as ligand precursor [32]. Reported herein is the synthesis, structure, solution behavior and ethylene polymerization of new malonate based enaminoketonato titanium and zirconium complexes.

2. Results and discussion

2.1. Synthesis and characterization of complexes *1Ti–3Ti* and *1Zr–2Zr*

A general synthetic route for the titanium **1Ti–3Ti** and zirconium **1Zr–2Zr** complexes is presented in Scheme 1. Ligand precursors **1–3** were prepared with chosen anile compounds using ethyl 3-ethoxy-3-imino-propionate hydrochloride as a starting material [33]. Corresponding complexes **1Ti–3Ti** and **1Zr–2Zr** were synthesized through lithium salts under mild conditions. The desired titanium complexes were obtained from toluene solutions as dark red powders while their zirconium analogues were light yellow. All the complexes were synthesized with reasonable yields (29–36%).

The light yellow crystals of the complex **1Zr** suitable for X-ray structure determination were grown from saturated toluene solution at −60 °C. The solid-state structure of this complex is shown in Fig. 1 and selected bond lengths and angles are given in Table 1. In solid state complex **1Zr** adopts distorted octahedral coordination around the metal center with *trans* oxygen atoms, *cis* nitrogen atoms and *cis* chlorine atoms. The Zr–N and Zr–O bond lengths resemble those of FI-catalysts reported by Fujita and coworkers [34]. This might indicate that in **1Zr** the oxygen is more anionic in nature whereas the bond between nitrogen and zirconium resembles more of coordination type of bonding.

2.2. Solution behavior of complexes *1Ti–3Ti* and *1Zr–2Zr*

It is known that complexes bearing (N,O)-type ligands can adopt different configurational isomers [20,24,35] as displayed in

* Corresponding author. Fax: +358 919150198.
E-mail address: timo.repo@helsinki.fi (T. Repo).

0022-328X/$ - see front matter © 2009 Elsevier B.V. All rights reserved.
doi:10.1016/j.jorganchem.2009.04.029

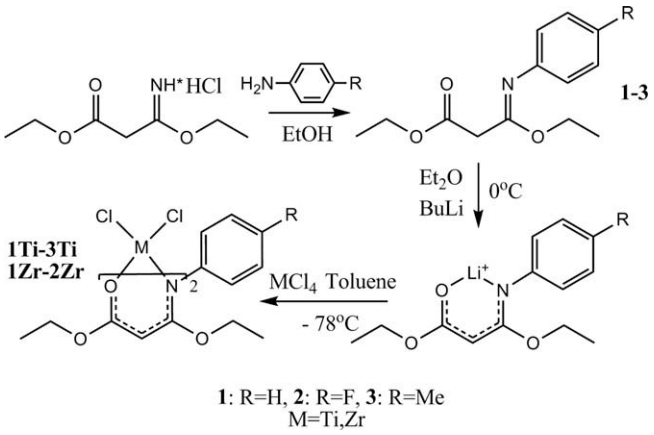

Scheme 1. Synthetic route for the complexes **1Ti**–**3Ti** and **1Zr**–**2Zr**.

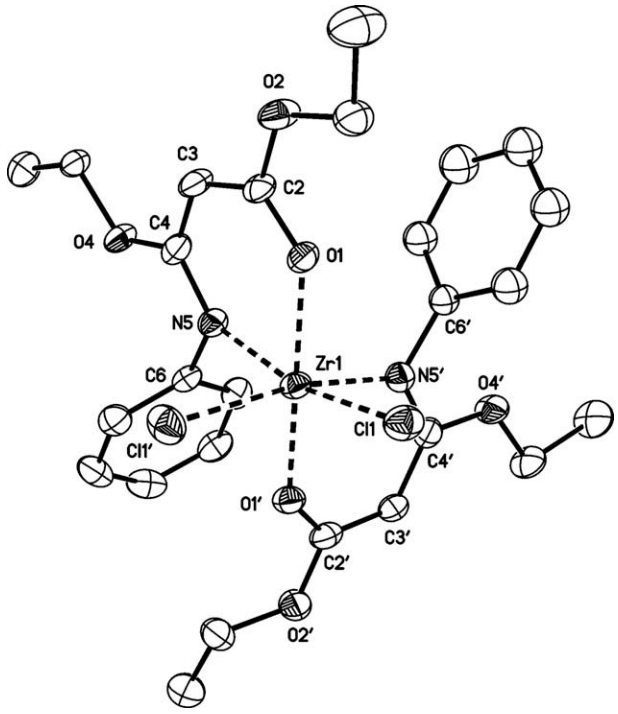

Fig. 1. Molecular structure of complex **1Zr** with thermal ellipsoids at 50% probability level. The solvent and all hydrogen atoms are omitted for clarity.

Table 1
Selected bond lengths and angles for complex **1Zr.**

Bond distances (Å)		Bond angles (°)	
Zr1–Cl1′	2.446(1)	O1–Zr–N5′	78.4(1)
Zr1–Cl1	2.463(1)	O1–Zr–N5′	95.5(1)
Zr1–N5′	2.235(3)	O1′–Zr–N5′	94.4(1)
Zr1–N5′	2.248(3)	O1′–Zr–N5′	78.52(1)
Zr1–O1’	2.072(3)	N5′–Zr–Cl1′	167.9(1)
Zr1–O1	2.069(3)	N5–Zr1–Cl1′	89.7(9)
O1′–C2′	1.288(5)	O1′–Zr1–Cl1	99.0(1)
O1–C2	1.285(5)	O1–Zr1–Cl1	88.0(1)
N5–C4	1.341(5)	N5′–Zr1–Cl1	88.9(1)
N5′–C4′	1.330(5)	Cl1–Zr1–Cl1′	93.75(4)
N5–C6	1.455(5)	O1–Zr1–O1′	170.6(1)
N5′–C6′	1.451(5)	N5–Zr1–N5′	90.5(1)

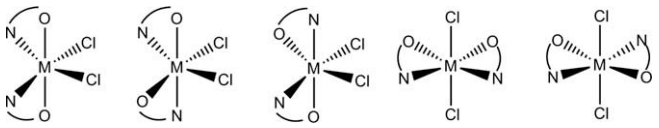

Scheme 2. Five different configurational isomers of (N,O)-type complexes.

Scheme 2. According to ^{1}H NMR the complexes have two different configurational isomeric structures in $CDCl_3$-solution, which can be seen from ^{1}H NMR spectrum of complex **1Zr** displayed in Fig. 2. These two isomers can be indentified from the two distinctive singlets, attributed to the CH-group in the molecule. Intensity ratios of these singlets are close to 1:2 favoring the isomer having CH-signal at lower field. Both configurational isomers have also two sets of CH_2 and CH_3 protons uprising from the ethoxide groups. With one of the isomers of complex **1Zr**, the rotation of phenyl ring is not hindered and CH_2-protons display clear quartet structures. In the other isomer structure the rotations of phenyl groups are hindered revealing complex set of aromatic proton signals and splitted metheine signals. ^{1}H-NMR of **1Zr** was measured also in a different, less polar, solvent d^8-toluene. Then the intensity ratio of the CH-signals was changed close to 1:4 again favoring the isomer having CH-signal at lower field. This phenomenon can be seen from the spectrum displayed in Fig. 3. These results underline the dynamic behavior of the complex in solution and dependence of balance between the isomers in different solvents.

To gain a more detailed understanding of the fluxional behavior of the complexes dynamic ^{1}H NMR (d^8-toluene) measurements were carried out. From Fig. 4 it can be seen that upon heating the two sets of peaks from CH_2 protons in the upper field become equivalent and also coalescence for the CH_2 protons in the lower field can be observed. The coalescence temperatures for the CH_2-protons are 25 °C and 5 °C and the corresponding energies for activation of rotation process are $\Delta G \neq (300.5\ K) = 14.8 \pm 0.9$ kcal mol^{-1} and $\Delta G \neq (288.2\ K) = 14.3 \pm 0.9$ kcal mol^{-1}. All the spectra are reversible within the studied temperature range. It should also be noted that the second isomeric structure of the complex, where the rotation of the phenyl ring is not hindered, is not affected by the temperature change.

The fluxuation phenomenon of the herein studied malonate based enaminoketonato complexes is noticeably different than some of the other (N,O)-type complexes published before [20,24,35]. With the complexes studied here no coalescence of chelating proton was observed. These results suggest that different isomers of malonate based enaminoketonato dichloro complexes are fairly stable in solution under the applied temperature scale. To verify that the isomers arise from different configurational structures and not from various intra- or intermolecular hydrogen bonding, NMR measurements in d-THF were carried out with complex **1Zr**. Presence of different isomers was observed also in these experiments, thus excluding plausible intra- or intermolecular hydrogen bonding [36].

2.3. Ethylene polymerization

Synthesized complexes were activated with MAO and used as catalysts for ethylene polymerization. The results of these experiments are listed in Table 2. Electron-withdrawing or -donating *para*-substituents were introduced onto coordinating imino group to study how the electronic properties influence the catalytic activities of the complexes. However, these substituents revealed only minor changes in polymerization activities of the catalysts. Of the five catalyst system studied, *para*-F substituted **2Zr**/MAO exhibited the highest catalytic activity of 104 kg PE/(mol$_{Zr}$ h bar). Correspondingly in the series of the titanium catalyst the *para*-F

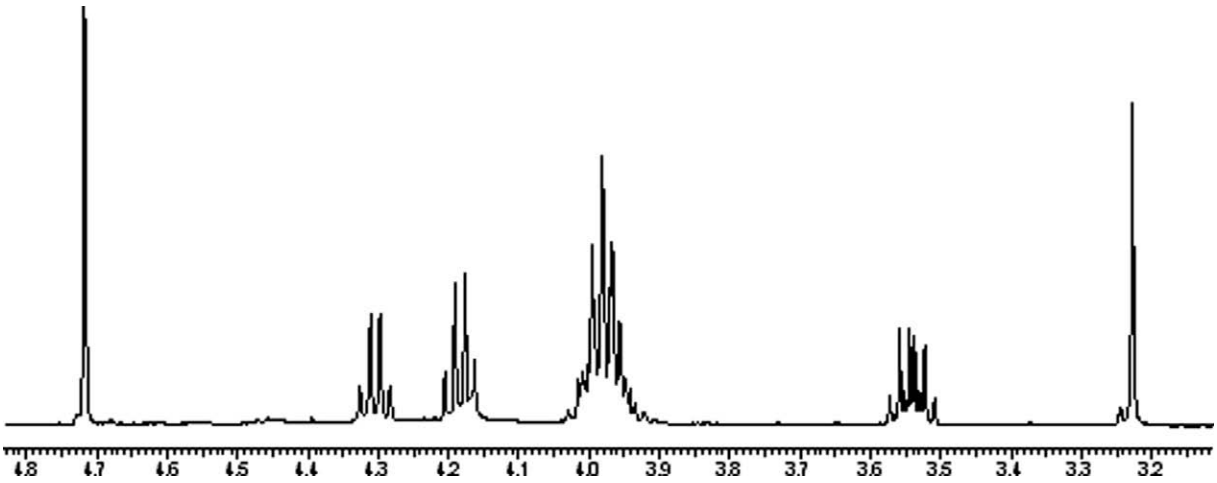

Fig. 2. ^{1}H NMR spectrum of complex **1Zr** measured in $CDCl_3$. Singlets attributed to CH protons in the molecule can be seen at 4.72 and 3.22 ppm. The other signals are attributed to CH_2 protons in the molecule.

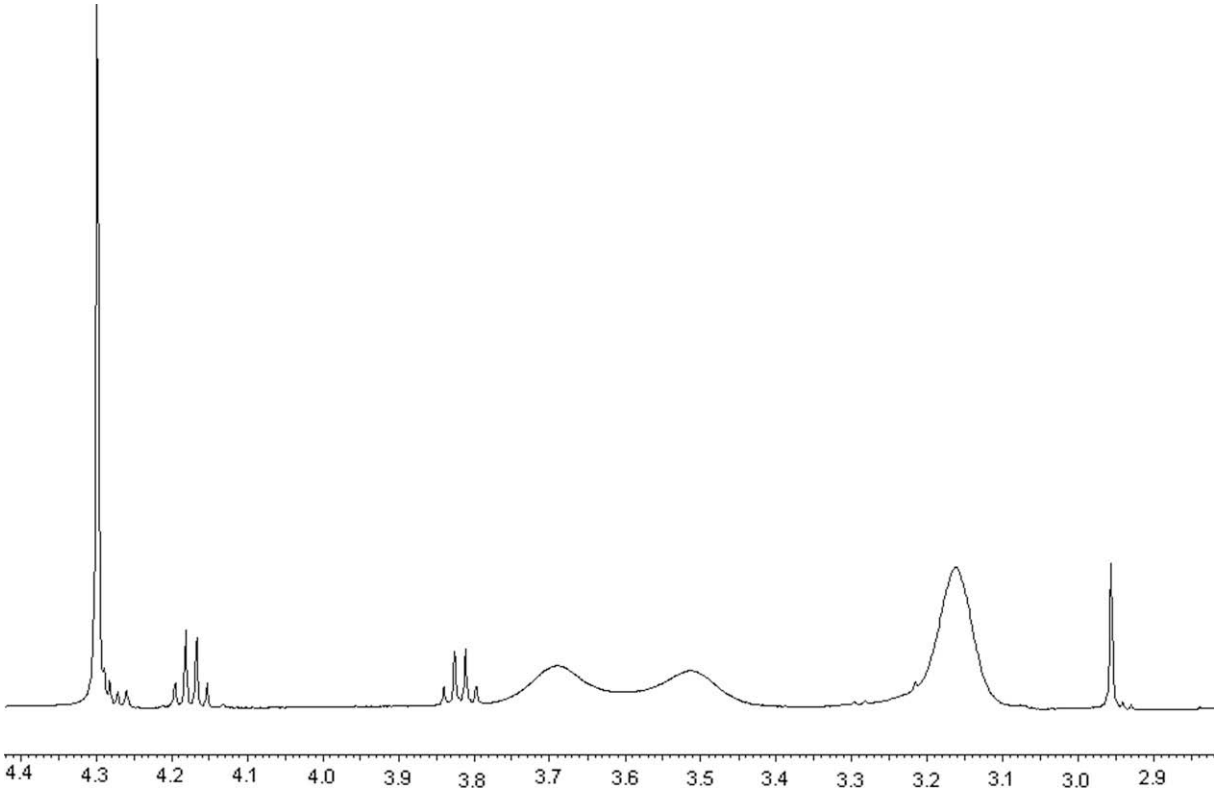

Fig. 3. ^{1}H NMR spectrum of complex **1Zr** measured in d^8-toluene. Singlets attributed to CH protons in the molecule can be seen at 4.30 and 2.95 ppm. The other signals are attributed to CH_2 protons in the molecule.

substituted **2Ti**/MAO turned out to be slightly more active than the *para*-Me and *para*-H substituted Ti-catalysts. The influence of *para*-substituents is similar as reported with related FI-catalyst family [37]. It seems that the electron-withdrawing *para*-F substituent enhances Lewis acidity of the titanium center. This results in an increase in a metal–carbon bond reactivity and reduced activation energy for ethylene insertion.

The nature of the *para*-substituent has also a marked effect on the thermal stability of titanium complexes. Catalyst **3Ti**/MAO, with the *para*-Me substituent, is thermally the most stable revealing highest activity at 60 °C. On the other hand, **2Ti**/MAO with *para*-F substituent is thermally the least stable one and consequently the polymerization activity is decreased when polymerization temperature is increased. Thermal stability of the Ti-catalysts corresponds with the above discussed reactivity of the metal–carbon bond. In general the zirconium catalysts seem to be more thermally stable then their titanium counterparts as the activity of **1Zr**/MAO and **2Zr**/MAO increases with increasing polymerization temperature.

The polyethylenes produced by **1Ti–3Ti**/MAO and **1Zr–2Zr**/MAO systems exhibit bi- or multimodal molecular weight distribution (MWD). This feature may be attributed to the dynamic nature of the used catalyst precursors as the molecular weights and the intensities of low- and high molecular weight part are depended

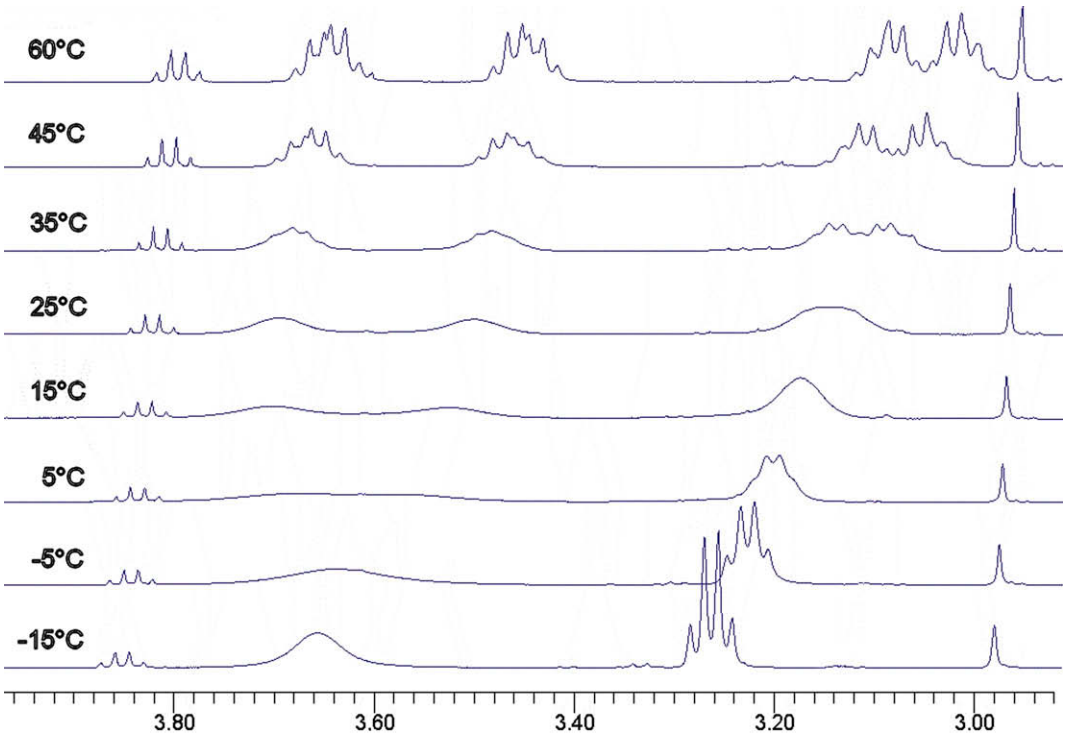

Fig. 4. Temperature variable NMR measurements with complex **1Zr** in d^8-toluene.

Table 2
Selected ethylene polymerization results with MAO-activated complexes **1Ti**–**3Ti** and **1Zr**–**2Zr**/MAO.

Run	Complex	T_p (°C)[a]	p (bar)[b]	Activity[c]	M_w (kg/mol)	M_w/M_n	T_m (°C)
1	**1Ti**	22	5	27	66/910	6.2	135
2	**1Ti**	30	5	66	40/708	8.4	136
3	**1Ti**	45	5	31	36/1230	Broad*	135
4	**1Ti**	60	5	26	34/430	15.1	138
5	**2Ti**	22	5	85	36/2370	Broad*	135
6	**2Ti**	30	5	59	33/2290	Broad*	137
7	**2Ti**	45	5	36	83/790	Broad*	137
8	**2Ti**	60	5	18	42/1000	Broad*	138
9	**3Ti**	22	5	34	3100	11.9	139
10	**3Ti**	30	5	22	63/1290	13.7	136
11	**3Ti**	45	5	29	71/1290	Broad*	135
12	**3Ti**	60	5	50	71/1020	7.3	135
13	**1Zr**	22	5	8	1.9/63/1860	Broad*	136
14	**1Zr**	30	5	25	2.5/59/1260	Broad*	138
15	**1Zr**	45	5	29	2.4/41/1320	Broad*	139
16	**1Zr**	60	5	45	51/1230	Broad*	138
17	**2Zr**	22	5	30	60/980	12.2	135
18	**2Zr**	30	5	34	71/830	6.0	135
19	**2Zr**	45	5	51	78/650	16.9	136
20	**2Zr**	60	5	104	76/650	9.2	136

Polymerization conditions: 20 μmol of catalyst, [Al]/[M] = 2000, polymerization time 30 min.
[a] Polymerization temperature.
[b] Monomer pressure.
[c] Activity in (kg PE)/(mol M h bar).
* Average M_w/M_n value over 20.

on the polymerization temperature. Depending on the temperature, high molecular weight part varies from 430 to 2400 kg/mol and the low molecular weight part from 33 to 83 kg/mol. With **1Zr**/MAO also formation of oligomers (Mw ~ 2000) was observed. According to the GPC results these catalysts produce polymers with relatively broad MWD values indicating non-single-site behavior. Also different molecular weight fractions may partly overlap with each other leading to broad molecular weight distribution values.

Even though the NMR experiments were carried out with dichloro complexes it is reasonable to expect that the fluxional features of the complexes reflects also to the MAO activated catalysts producing bi- and multimodal polyethylenes, as described for other related catalysts [20,35,38]. It is noteworthy that related enaminoketonato catalysts based on acetylacetonato backbone do not produce multimodal polyethylenes [22–24]. This indicates that the ethoxy group in herein studied catalysts has an effect on their catalytic performance. It might cause the multimodality of

the polymers through fluxionality in catalytically active species or it may have indirect influence. For example the reactions between the catalyst structure and MAO may be enhanced leading to formation of multiple active sites [34,35].

3. Conclusions

Five new Group IV metal complex (**1Ti–3Ti** and **1Zr–2Zr**) bearing malonate based enaminoketonato ligands have been synthesized and characterized. When activated with MAO the complexes displayed relatively low activities of 8–104 $kg_{PE}/(mol_M\ h\ bar)$ in ethylene polymerizations the *para*-F substituted catalysts being the most active. The GPC results revealed that none of the produced polymers were unimodal and that the intensities of different molecular weight fractions were depended on both catalyst and used polymerization conditions. These results indicate that the MAO activated catalysts **1Ti–3Ti and 1Zr–2Zr** have more than one active center and that each of these active centers respond differently when polymerization conditions are altered. Even though no conclusive answer for this behavior can be given at the moment, it is possible that the multimodality is a consequence of fluxionality identified by ^{1}H-NMR in herein studied complexes.

4. Experimental section

All complex syntheses and polymerization experiments were performed under argon atmosphere using standard Schlenk techniques. Solvents for complex synthesis (diethylether and toluene, HPLC grade) were dried over sodium flakes and distilled before use. Solvents for synthesis of ligand precursors (ethanol and chloroform, HPLC grade) were used as received. $TiCl_4$ was purchased from Fluka and $ZrCl_4$ from Aldrich. Both were used as received. Other reagents of high purity grade were purchased from commercial sources and used as received. MAO (30% in toluene) was obtained from Borealis Polymers Ltd.

Polymerization experiments were conducted in 1-L Büchi steel autoclave. Autoclave was charged with 200 mL of dry toluene, cocatalyst (MAO) and heated to desired temperature. Autoclave was saturated with ethylene and polymerization was initiated by addition of precatalyst solution. The monomer pressure, temperature and monomer consumption were controlled by real-time monitoring. Polymerization was quenched with 10% HCl solution in methanol, polymer was precipitated quantitatively by pouring the solution into methanol (400 mL), acidified with a small amount of HCl. Obtained polymer was washed several times with methanol and water followed by drying at 60 °C.

NMR spectra were recorded in $CDCl_3$ or in d^8-toluene at 25 °C on a Varian Gemini 200 spectrometer operating at 200 MHz (^{1}H NMR) and 50.286 MHz (^{13}C NMR). Dynamic NMR spectra were recorded with Varian Unity Inova spectrometers operating at 500 MHz. Elemental analyses were performed with an EA 1110 CHNS-O CE instrument. Molecular weights and molecular weight distributions of polyethylene samples were determined with a Waters Alliance GPCV 2000 high temperature gel chromatographic device. HMW7, 2* HMWGE, and HMW2 Waters Styrogel columns were used for GPC. Measurements were performed in 1,2,4-trichlorobentzene (TCB) at 160 °C relative to polyethylene standards, and 2,6-di-*tert*-butyl-4-methylphenol was used as a stabilizer. Chromatograms were calibrated using linear polystyrene standards. DSC measurements were performed on a Perkin–Elmer DSC, calibrated with indium (temperature scanning 10 °C/min). Scan area from 25 °C to 232 °C.

4.1. Preparation of [EtOC(O)CH_2C(NPh)EtO] **1**

Ethyl-3-ethoxy-3-(phenylimino)-propanoate, **1**, was prepared according to a known literature procedure [32]. 25.56 mmol (5.0 g) of ethyl 3-ethoxy-3-imino-propionate hydrochloride was added to an ethanol solution of aniline (25.56 mmol, 2.38 g). Reaction mixture was stirred overnight at room temperature followed by filtration. The remaining solid material was washed with ethanol, filtrates were combined, slurried in chloroform and filtered again. Liquid product was purified by vacuum distillation. Yield 4.12 g (70%). ^{1}H NMR ($CDCl_3$, 200 MHz, 302 K): δ = 7.25 (m, 2H, Ar); 7.02 (m, 1H, Ar); 6.77 (m, 2H, Ar); 4.26 (q, 2H, –O–CH_2-Me); 4.12 (q, 2H, –O–CH_2–Me); 3.17 (s, 2H, –(CO)–CH_2–(CN)–); 1.32 (t, 3H, –CH_3); 1.22 (t, 3H, –CH_3) ^{13}C{^{1}H NMR}($CDCl_3$, 50.3 MHz, 302 K): δ = 167.9 (*C*═N), 156.5 (*C*═O), 148.2 (–N-*Ar*), 129.0 (*Ar*), 123.3 (*Ar*), 121.0 (*Ar*), 62.1 (–O–CH_2–), 61.2 (–O–CH_2–), 36.4 –[(CO)–CH_2–(CN)–], 14.2 (*C*H_3), 14.0 (*C*H_3) Anal. Calc. for $C_{13}H_{17}NO_3$: C, 66.36; H 7.28; N, 5.95; found C, 66.84; H 6.71; N, 5.80.

4.2. Preparation of EtOC(O)CH_2C(N(p-F-Ph))EtO] **2**

Compound **2** was prepared by a similar method to that described for **1** with 74% yield. ^{1}H NMR ($CDCl_3$, 200 MHz, 302 K): δ = 6.97 (m, 2H, Ar); 6.78 (m, 2H, Ar); 4.27 (q, 2H, –O–CH_2-Me); 4.15 (q, 2H, –O–CH_2-Me); 3.19 (s, 2H, –(CO)–CH_2–(CN)–); 1.34 (t, 3H, –CH_3,); 1.25 (t, 3H, –CH_3) ^{13}C{^{1}H NMR}($CDCl_3$, 50.3 MHz, 302 K): δ = 167.7 (*C*═N), 161.6 (*Ar*-F), 157.1 (*Ar*-F), 156.9 (*C*═O), 144.2 (N-*Ar*), 143.9 (N-*Ar*) 122.4 (*Ar*), 122.2 (*Ar*), 115.8 (*Ar*), 115.4 (*Ar*), 62.1 (–O–CH_2–), 61.3 (–O–CH_2–), 36.3 –[(CO)–CH_2–(CN)–], 14.1 (*C*H_3), 14.0 (*C*H_3) Anal. Calc. for $C_{13}H_{16}FNO_3$: C, 61.65; H, 6.37; N, 5.53; found C, 61.84; H, 6.71; N, 5.36.

4.3. Preparation of EtOC(O)CH_2C (N(p-Me-Ph))EtO] **3**

Compound **3** was prepared by a similar method to that described **1** with 67% yield. ^{1}H NMR ($CDCl_3$, 200 MHz, 302 K): δ = 7.07 (m, 2H, Ar); 6.88 (m, 2H, Ar); 4.26 (q, 2H, –O–CH_2-Me); 4.12 (q, 2H, –O–CH_2-Me); 3.19 (s, 2H, –(CO)–CH_2–(CN)–); 2.29 (s, 3H, Ar-CH_3); 1.32 (t, 3H, –CH_3,); 1.24 (t, 3H, –CH_3) ^{13}C{^{1}H NMR}($CDCl_3$, 50.3 MHz, 302 K): δ = 167.8 (*C*═N), 156.4 (*C*═O), 145.5 (–N-*Ar*), 132.4 (*Ar*-Me), 129.5 (*Ar*), 120.7 (*Ar*), 61.9 (–O–CH_2–), 61.1 (–O–CH_2–), 36.2 –[(CO)–CH_2–(CN)–], 20.6 (Ar-CH_3), 14.1 (–O–CH_2–CH_3), 14.0 (–O–CH_2–CH_3) Anal. Calc. for $C_{14}H_{19}NO_3$: C, 67.45; H, 7.68; N, 5.62; found C, 67.74; H, 7.71; N, 5.58.

4.4. Preparation of [EtOC(O)CHC(NPh)EtO]$_2$$TiCl_2$ **1Ti**

n-Butyllithium (1.6 M, 8.5 mmol, 5.3 mL) was added dropwise to a stirred solution of **1** (8.5 mmol, 2.0 g) in dried Et_2O (40 mL) at 0 °C. The solution was allowed to warm to room temperature and stirred for 5 h. After removal of the solvent under vacuum the formed lithium-salt was solvated to precooled (−78 °C) toluene (50 ml) and added dropwise to a precooled (−78 °C) toluene (30 ml) solution of $TiCl_4$ (4.25 mmol, 0.81 g). The reaction mixture was warmed to ambient temperature and stirred overnight. The formed product was filtered through Celite followed by removal of solvent under vacuum. Recrystallization from toluene gave desired complex **1Ti** as a dark red powder in a 31% yield. ^{1}H NMR ($CDCl_3$, 200 MHz, 302 K): δ = 7.30–7.24 (m, 2H, Ar); 7.07–6.88 (m, 6H, Ar); 6.82–6.72 (m, 2H, Ar); 4.16 (s, 1H, –(CO)–C*H*–(CN)–); 4.26 (q, 2H, –O–CH_2-Me); 4.14 (q, 2H, –O–CH_2-Me); 3.94 (m, 3H, –O–CH_2-Me); 3.51 (m, 1H, –O–CH_2-Me) 3.18 (s, 1H –(CO)–C*H*–(CN)–); 1.33 (t, 3H, –CH_3,); 1.24 (t, 3H, –CH_3); 1.14 (t, 3H, –CH_3); 1.10 (t, 3H, –CH_3) ^{13}C{^{1}H NMR}($CDCl_3$, 50.3 MHz, 302 K): δ

= 169.5 (*C*═N), 168.1 (*C*═N), 168.9 (*C*═O), 156.5 (*C*═O), 148.3 (–N-*Ar*), 148.2 (–N-*Ar*), 129.1 (*Ar*), 127.8 (*Ar*), 126.9 (*Ar*), 125.1 (*Ar*), 123.5 (*Ar*), 121.2 (*Ar*), 75.5 [–(CO)–*C*H–(CN)–], 65.2 (–O–*C*H_2–), 62.8 (–O–*C*H_2–), 62.2 (–O–*C*H_2–), 61.2 (–O–*C*H_2–), 36.6 [–(CO)–*C*H–(CN)–], 14.3 (*C*H_3), 14.2 (*C*H_3), 14.1 (*C*H_3), 14.0 (*C*H_3) Anal. Calc. for $C_{26}H_{32}N_2O_6TiCl_2$: C, 53.17; H, 5.49; N, 4.77; found C 53.01; H, 5.38; N, 4.61.

4.5. Preparation of [EtOC(O)CHC(N(p-F-Ph)EtO]$_2$TiCl$_2$ **2Ti**

Complex **2Ti** was prepared by a similar method to that described for **1Ti** with yield of 29%. ^{1}H NMR ($CDCl_3$, 200 MHz, 302 K): δ = 7.08–6.79 (m, 6H, Ar); 6.82–6.72 (m, 2H, Ar); 4.15 (s, 1H, –(CO)–*C*H–(CN)–); 4.25 (q, 2H, –O–*C*H_2-Me); 4.16 (q, 2H, –O–*C*H_2-Me); 3.94 (m, 3H, –O–*C*H_2-Me); 3.49 (m, 1H, –O–*C*H_2-Me) 3.18 (s, 1H-(CO)–*C*H–(CN)–); 1.32 (t, 3H, –*C*H_3); 1.25 (t, 3H, –*C*H_3); 1.15 (t, 3H, –*C*H_3); 1.11 (t, 3H, –*C*H_3) ^{13}C{^{1}H NMR}($CDCl_3$, 50.3 MHz, 302 K): δ = 170.6 (*C*═N), 169.9 (*C*═O), 167.8 (*C*═N), 163.0 (*Ar*-F), 161.6 (*Ar*-F), 158.2 (*Ar*-F), 157.2 (*Ar*-F), 156.9 (*C*═O), 144.2 (N-*Ar*), 143.7(N-*Ar*), 139.2 (N-*Ar*), 139.0 (N-*Ar*), 122.5 (*Ar*), 122.2 (*Ar*), 116.4 (*Ar*), 115.9(*Ar*), 115.8 (*Ar*), 115.4 (*Ar*), 115.2 (*Ar*), 114.8 (*Ar*), 70.2 [–(CO)–*C*H–(CN)–], 65.3 (–O–*C*H_2–), 62.4 (–O–*C*H_2–), 62.1 (–O–*C*H_2–), 61.5 (–O–*C*H_2–), 36.5 [–(CO)–*C*H–(CN)–], 14.2 (*C*H_3), 14.1 (*C*H_3), 14.1 (*C*H_3), 14.0 (*C*H_3) Anal. Calc. for $C_{26}H_{30}N_2O_6F_2TiCl_2$: C, 50.10; H, 4.85; N, 4.49; found C, 49.81; H, 4.78; N, 4.38.

4.6. Preparation of [EtOC(O)CHC(N(p-Me-Ph)EtO]$_2$TiCl$_2$ **3Ti**

Complex **3Ti** was prepared by a similar method to that described for **1Ti** with yield of 34%. ^{1}H NMR ($CDCl_3$, 200 MHz, 302 K): δ = 6.98–6.81 (m, 6H, Ar); 6.61–6.69 (m, 2H, Ar); 4.17 (s, 1H, –(CO)–*C*H–(CN)–); 4.25 (q, 2H, –O–*C*H_2–Me); 4.18 (q, 2H, –O–*C*H_2-Me); 3.92 (m, 3H, –O–*C*H_2-Me); 3.52 (m, 1H, –O–*C*H_2-Me) 3.20 (s, 1H –(CO)–*C*H–(CN)–); 1.33 (t, 3H, –*C*H_3); 1.24 (t, 3H, –*C*H_3); 1.15 (t, 3H, –*C*H_3); 1.11 (t, 3H, –*C*H_3) ^{13}C{^{1}H NMR}($CDCl_3$, 50.3 MHz, 302 K): δ = 169.4 (*C*═N), 168.0 (C═N), 168.8 (*C*═O), 156.8 (C═O), 145.7 (–N-*Ar*), 145.3 (–N-Ar), 134.5 (*Ar*-Me), 132.4 (Ar), 129.7 (Ar), 129.6 (*Ar*), 126.2 (*Ar*), 120.7 (Ar), 75.6 [–(CO)–*C*H–(CN)–], 65.2 (–O–*C*H_2–), 62.7 (–O–*C*H_2–), 61.8 (–O–*C*H_2–), 61.2 (–O–*C*H_2–), 36.4 [–(CO)–*C*H–(CN)–], 20.9 (Ar-*C*H_3), 20.7 (Ar-*C*H_3), 14.2 (*C*H_3), 14.1(7) (*C*H_3), 14.1(1) (*C*H_3), 14.0(*C*H_3) Anal. Calc. for $C_{28}H_{36}N_2O_6TiCl_2$: C, 54.65; H, 5.90; N, 4.55; found C, 54.80; H, 5,98; N, 4.50.

4.7. Preparation of [EtOC(O)CHC(NPh)EtO]$_2$ZrCl$_2$ **1Zr**

Complex **1Zr** was prepared by a similar method to that described for **1Ti** with yield of 36%. ^{1}H NMR ($CDCl_3$, 200 MHz, 302 K): δ = 7.29–7.20 (m, 2H, Ar); 7.05–6.92 (m, 6H, Ar); 6.86–6.74 (m, 2H, Ar); 4.72 (s, 1H, –(CO)–*C*H–(CN)–); 4.27 (q, 2H, –O–*C*H_2–Me); 4.16 (q, 2H, –O–*C*H_2-Me); 3.96 (m, 3H, –O–*C*H_2-Me); 3.48 (m, 1H, –O–*C*H_2-Me) 3.22 (s, 1H–(CO)–*C*H–(CN)–); 1.35 (t, 3H, –*C*H_3,); 1.27 (t, 3H, –*C*H_3); 1.14 (t, 3H, –*C*H_3); 1.10 (t, 3H, –*C*H_3) ^{13}C{^{1}H NMR}($CDCl_3$, 50.3 MHz, 302 K): δ = 170.1 (*C*═N), 168.4 (*C*═N), 156.5 (*C*═O), 156.4 (*C*═O), 148.3 (–N-*Ar*), 148.2 (–N-*Ar*), 129.1 (*Ar*),129.0 (*Ar*), 128.1 (*Ar*), 125.2 (*Ar*), 123.5 (*Ar*), 121.2 (*Ar*), 70.1 [–(CO)–*C*H–(CN)–], 65.0 (–O–*C*H_2–), 62.2 (–O–*C*H_2–), 62.1 (–O–*C*H_2–), 61.2 (–O–*C*H_2–), 36.7 [–(CO)–*C*H–(CN)–], 14.2 (*C*H_3), 14.1(8) (*C*H_3), 14.1(1) (*C*H_3), 14.0 (*C*H_3) Anal. Calc. for $C_{26}H_{32}N_2O_6ZrCl_2$: C, 49.52; H, 5.11; N, 4.44; found C, 49.81; H, 5.26; N, 4.36.

4.8. Preparation of [EtOC(O)CHC(N(p-F-Ph)EtO]$_2$ZrCl$_2$ **2Zr**

Complex **2Zr** was prepared by a similar method to that described for **1Ti** with yield of 32%. ^{1}H NMR ($CDCl_3$, 200 MHz, 302 K): δ = 7.05–6.82 (m, 6H, Ar); 6.82–6.72 (m, 2H, Ar); 4.72 (s, 1H, –(CO)–*C*H–(CN)–); 4.27 (q, 2H, –O–*C*H_2-Me); 4.16 (q, 2H, –O–*C*H_2-Me); 3.96 (m, 3H, –O–*C*H_2-Me); 3.54 (m, 1H, –O–*C*H_2-Me) 3.19 (s, 1H –(CO)–*C*H–(CN)–); 1.35 (t, 3H, –*C*H_3,); 1.27 (t, 3H, –*C*H_3); 1.15 (t, 3H, –*C*H_3); 1.10 (t, 3H, –*C*H_3) ^{13}C{^{1}H NMR}($CDCl_3$, 50.3 MHz, 302 K): δ = 170.8 (*C*═N), 169.4 (*C*═O), 167.5 (*C*═N), 163.2 (*Ar*-F), 161.5 (*Ar*-F), 158.4 (*Ar*-F), 157.1 (*Ar*-F), 156.9 (*C*═O), 144.0 (N-*Ar*), 143.7(N-*Ar*), 139.2 (N-*Ar*), 139.1 (N-*Ar*), 122.5 (*Ar*), 122.0 (*Ar*), 116.3 (*Ar*), 115.9(*Ar*), 115.6 (*Ar*), 115.5 (*Ar*), 115.1 (*Ar*), 114.8 (*Ar*), 70.8 [–(CO)–*C*H–(CN)–], 65.5 (–O–*C*H_2–), 62.5 (–O–*C*H_2–), 62.3 (–O–*C*H_2–), 61.4 (–O–*C*H_2–), 36.4 [–(CO)–*C*H–(CN)–], 14.2 (*C*H_3), 14.2 (*C*H_3), 14.1 (*C*H_3), 14.0 (*C*H_3) Anal. Calc. for $C_{26}H_{30}N_2O_6F_2ZrCl_2$: C, 46.84, H 4.54, N, 4.20; found C, 46.95; H, 4.63; N, 4.14.

4.9. X-ray Crystallographic Study of **1Zr**

The single-crystal X-ray diffraction study of **1Zr** was carried out on a Bruker–Nonius Kappa-CCD diffractometer at 123(2) K using Mo Kα radiation (α = 0.71073 Å). Direct Methods (SHELXS-97) were used for structure solution, and full-matrix least-squares refinement on F^2 (SHELXL-97). [39] H atoms were localized by difference Fourier synthesis and refined using a riding model. A semi-empirical absorption correction was applied.

1Zr: yellow crystals, $C_{27}H_{32}Cl_2N_2O_6Zr$ – 0.5 C_7H_8, M = 676.72, crystal size 0.36 × 0.20 × 0.04 mm, monoclinic, space group $P2_1/n$ (No. 14): a = 12.204(2) Å, b = 14.905(3) Å, c = 17.401(4) Å, β = 90.65(2) V = 3165.0(11) Å^3, Z = 4, ρ(calc.) = 1.420 Mg m^{-3}, F(0 0 0) = 1396, ρ = 0.559 mm^{-1}, 36922 reflexes ($2\theta_{max}$ = 50°), 5572 unique [R_{int} = 0.080], 328 parameters, 19 restraints, R1 ($I > 2\sigma(I)$) = 0.045, *wR2* (*all data*) = 0.106, GooF = 1.06, largest diff. peak and hole 0.697 and −0.526e Å^{-3}.

Acknowledgements

Financial support for this work from Academy of Finland, Projects 209739 and 123248 is greatly acknowledged. Warm thanks to Doctor Sami Hietala and Sirpa Vuorinen for the help with dynamic NMR measurements. Warm thanks also to Sami Lipponen for the help with GPC measurements of the polymer products.

Appendix A. Supplementary data

Supplementary data associated with this article can be found, in the online version, at doi:10.1016/j.jorganchem.2009.04.029.

CCDC 716356 contains the supplementary crystallographic data for complex **1Zr**. These data can be obtained free of charge from The Cambridge Crystallographic Data Centre via www.ccdc.cam.ac.uk/data_request/cif.

References

[1] S.D. Ittel, L.K. Johnson, M. Brookhart, Chem. Rev. 100 (2000) 1169.
[2] G.J.P. Britovsek, V.C. Gibson, D.F. Wass, Angew. Chem. Int. Ed. 38 (1999) 428.
[3] V.C. Gibson, S.K. Spitzmesser, Chem. Rev. 103 (2003) 283.
[4] R. Furuyama, T. Fujita, S.F. Funaki, T. Nobori, T. Nagata, K. Fujiwara, Catal. Surv. Asia 8 (2004) 61.
[5] H. Makio, N. Kashiwa, T. Fujita, Adv. Synth. Catal. 344 (2002) 477.
[6] L. Bourget-Merle, M.F. Lappert, J.R. Severn, Chem. Rev. 102 (2002) 3031.
[7] C. Qi, S. Zhang, J. Sun, J. Organomet. Chem. 690 (2005) 2941.
[8] M. Tamm, S. Randoll, E. Herdtweck, N. Kleigrewe, G. Kehr, G. Erker, B. Rieger, Dalton Trans. (2006) 459.
[9] M. Sanz, M.E.G. Mosquera, T. Cuenca, C. Ramírez de Arellano, B.M. Schormann, B. Bochmann, Polyhedron 26 (2007) 5339.
[10] M. Zhou, H. Tong, X. Wei, D. Liu, J. Organomet. Chem. 692 (2007) 5195.
[11] R.K.J. Bott, M. Hammond, P.N. Horton, S.J. Lancaster, M. Bochmann, P. Scott, Dalton Trans. (2005) 3611.
[12] M.J. Ferreira, I. Matos, T. Duarte, M. Marques, A.M. Martins, Catal. Today 647 (2008) 122.

[13] R.J. Long, V.C. Gibson, A.J.P. White, D.J. Williams, Inorg. Chem. 45 (2) (2006) 511.
[14] I. Kim, Y. Nishihara, R.F. Jordan, Organometallics 16 (1997) 3314.
[15] S. Chen, X. Zhang, H. Ma, Y. Lu, Z. Zhang, H. Li, X. Lu, N. Cui, Y. Hu, J. Organomet. Chem. 690 (2005) 4184.
[16] M. Said, D.L. Hughes, M. Bochmann, Inorg. Chim. Acta 359 (2006) 3467.
[17] Y. Yoshida, S. Matsui, T. Fujita, J. Organomet. Chem. 690 (2005) 4382.
[18] Y. Suzuki, H. Tanaka, T. Oshiki, K. Takai, T. Fujita, Chem. Asian J. (2006) 878.
[19] L.M. Tang, Y.Q. Duan, X.F. Li, Y.S. Li, J. Organomet. Chem. 691 (2006) 2023.
[20] Y. Tohi, H. Makio, S. Matsui, M. Onda, T. Fujita, Macromolecules 36 (2003) 523.
[21] Y. Tohi, T. Nakano, H. Makio, S. Matsui, T. Fujita, T. Yamaguchi, Macromol. Chem. Phys. 205 (2004) 1179.
[22] M. Tang Li, T. Hu, Y.J. Bo, Y.S. Li, N.H. Hu, J. Organomet. Chem. 690 (2005) 3125.
[23] X.-F. Li, K. Dai, W.P. Ye, L. Pan, Y.S. Li, Organometallics 23 (2004) 1223.
[24] W.P. Ye, J. Zhan, L. Pan, N.H. Hu, Y.S. Li, Organometallics 27 (2008) 3642.
[25] A. Sakuma, M.S. Weiser, T. Fujita, Polym. J. 39 (2007) 193.
[26] J.B. Edson, Z. Wang, E.J. Kramer, G.W. Coates, J. Am. Chem. Soc. 130 (2008) 4968.
[27] L.M. Tang, Y.G. Li, W.P. Ye, Y.S. Li, J. Polym. Sci. Part A: Polym. Chem. 44 (2006) 5846.
[28] R. Furuyama, M. Mitani, J. Mohri, R. Mori, H. Tanaka, T. Fujita, Macromolecules 38 (2005) 1546.
[29] J. Saito, Y. Suzuki, H. Makio, H. Tanaka, M. Onda, T. Fujita, Macromolecules 39 (2006) 4023.
[30] T. Matsugi, T. Fujita, Chem. Soc. Rev. 37 (2008) 1264.
[31] K. Oocuhi, M. Mitani, M. Hayakawa, T. Yamada, Macromol. Chem. Phys. 197 (1996) 1545.
[32] A. Pärssinen, P. Elo, M. Klinga, M. Leskelä, T. Repo, Inorg. Chem. Commun. 9 (2006) 859.
[33] N. Harris, Synthesis (1979) 826.
[34] S. Matsui, M. Mitani, J. Saito, Y. Tohi, H. Makio, N. Matsukawa, Y. Takagi, K. Tsuru, M. Nitabaru, T. Nakano, H. Tanaka, N. Kashiwa, T. Fujita, J. Am. Chem. Soc. 123 (2001) 6847.
[35] A. Parssinen, T. Luhtanen, M. Klinga, T. Pakkanen, M. Leskela, T. Repo, Organometallics 26 (2007) 3690.
[36] J. Moussa, C. Guyard-Duhayon, P. Herson, H. Amouri, Organometallics 23 (2004) 6231.
[37] S.-i. Ishii, J. Saito, M. Mitani, J.-i. Mohri, N. Matsukawa, Y. Tohi, S. Matsui, N. Kashiwa, T. Fujita, J. Mol. Catal. A: Chem. 179 (2002) 11.
[38] H. Makio, T. Fujita, Macromol. Symp. 213 (2004) 221.
[39] G.M. Sheldrick, Acta Crystallogr. A64 (2008) 112.